

# Investigations on variation of defects in fused silica with different annealing atmospheres using positron annihilation spectroscopy



Lijuan Zhang<sup>a,\*</sup>, Jing Chen<sup>a</sup>, Yilan Jiang<sup>a</sup>, Jiandang Liu<sup>b</sup>, Bingchuan Gu<sup>b</sup>, Xiaolong Jiang<sup>a</sup>, Yang Bai<sup>a</sup>, Chuanchao Zhang<sup>a</sup>, Haijun Wang<sup>a</sup>, Xiaoyu Luan<sup>a</sup>, Bangjiao Ye<sup>b</sup>, Xiaodong Yuan<sup>a</sup>, Wei Liao<sup>a,\*</sup>

<sup>a</sup> Research Center of Laser Fusion, China Academy of Engineering Physics, Mianyang 621900, China

<sup>b</sup> State Key Laboratory of Particle Detection and Electronics (IHEP & USTC), Department of Modern Physics, University of Science and Technology of China, Hefei 230026, China

## ARTICLE INFO

### Article history:

Received 18 April 2017

Received in revised form

10 June 2017

Accepted 24 June 2017

Available online 2 July 2017

### Keywords:

Fused silica

Positron annihilation

Thermal annealing

## ABSTRACT

The laser damage resistance properties of the fused silica can be influenced by the microstructure variation of the atom-size intrinsic defects and voids in bulk silica. Two positron annihilation spectroscopy techniques have been used to investigate the microstructure variation of the vacancy clusters and the structure voids in the polishing redeposition layer and the defect layer of fused silica after annealing in different atmospheres. The fused silica samples were isothermally annealed at 1000 K for 3 h in a furnace under an air atmosphere, a vacuum atmosphere and a hydrogen atmosphere, respectively. The positron annihilation results show that ambient oxygen atmosphere only affects the surface of the fused silica (about 300 nm depth) due to the large volume and low diffusion coefficient of the oxygen atom. However, hydrogen atoms can penetrate into the defect layer inside the fused silica and then have an influence on vacancy defects and vacancy clusters, while having no effect on the large voids. Besides, research results indicate that an annealing process can reduce the size and concentration of vacancy clusters. The obtained data can provide important information for understanding the laser damage mechanism and improving laser damage resistance properties of the fused silica optics.

© 2017 Elsevier B.V. All rights reserved.

## 1. Introduction

Because of its excellent optical properties, fused silica has been widely used for transmissive optics in inertial confinement fusion (ICF) facilities such as the National Ignition Facility (NIF), the Laser MegaJoule (LMJ) and the SG-III laser facility [1–3]. High power laser-induced damage (LID) in fused silica has attracted extensive scientific research interests since it extremely restricts the output of the large laser system. A number of studies have showed that subsurface damage (SSD) includes micro-flaws and mechanical scratches resulting from grinding and polishing treatments are responsible for laser damage initiation at 351/355 nm of fused silica. The removal of these precursors induces an increase of the laser-induced damage threshold [4]. Due to the fabrication process

and the impurities in raw materials and the other well-known factors, the actually formed structure will deviated from the perfect random network structure of  $\text{Si}(\text{O}_{1/2})_4$  tetrahedron. Breakage of Si–O covalent bond, loss of oxygen ions and oxygen/silicon interstitials are observed in pure fused silica. The intrinsic microstructural point defects associated with non-bridging oxygen hole centers (NBOHC) and oxygen deficient centers (ODC) have also been found to have direct relations to LID in fused silica [5–7]. The formation and the spatial distribution of the NBOHC and ODC defects about the  $3\omega$  laser damage initiation crater in fused silica has been determined by Wong et al. [8]. Kucheyev and Demos [9] have investigated an increase in the concentration of NBOHC and ODC defects after high fluence laser irradiation. Exposure of fused silica to high fluence UV (355 nm) laser leads to Si/O stoichiometry variation as well as to the formation of ODC defects in fused silica [10].

A conventional method of removing point defects is to thermally anneal the material in a furnace. Shen et al. [11] have pointed out that only relatively modest temperatures (approximately 400 °C)

\* Corresponding authors. 64 Mianshan Road, Youxian District, Mianyang 621900, China.

E-mail addresses: [ljjzhang105@163.com](mailto:ljjzhang105@163.com) (L. Zhang), [liaowei@caep.cn](mailto:liaowei@caep.cn) (W. Liao).

and times are required to anneal out isolated point defects. The damage threshold on indentation improves from 8 to 35 J/cm<sup>2</sup> after annealing at approximately 750 °C. Thus, investigation of defects variation under different annealing processes is very important in improving laser damage resistance properties of the fused silica optics.

The laser damage resistance properties of the fused silica can be influenced by the microstructure variation of the atom-size intrinsic defects and voids in bulk silica. It is very difficult to non-destructively characterize the tiny atomic size modifications of intrinsic defects and voids in thermally treatment of high quality fused silica. Positron annihilation spectroscopy (PAS) technique is a powerful method and sensitive to study such nanometer-scaled open spaces such as vacancy-type defects in metals, free volumes in polymers, and voids in oxides [12–15]. Positrons tend to localize at open spaces in these materials and annihilate with the surrounding electrons [16–18]. Positron in the silica glass can form positronium (Ps), a bound state of a positron and an electron. Ps exists in two spin states, the short-lived para- positronium (p-Ps) and the long-lived ortho- positronium (o-Ps). Ps is formed for 25% in the antiparallel spin singlet state, p-Ps, and for 75% in the spin triplet state, o-Ps [19]. These states have a vacuum lifetimes of 125 ps and 140 ns, respectively. The p-Ps lifetime in a-SiO<sub>2</sub> was found to be 156 ± 4 ps. This was because that the screening of the Coulomb interaction between the constituent particles by electrons of the medium and that the average distance between the electron and positron in positronium becomes larger than its vacuum value [20]. The o-Ps lifetime is shortened to the order of a few nanoseconds in a void of the matter by the so called pick-off process. In particular, about 80% of positrons form Ps in silica glass (SiO<sub>2</sub>); the Ps is localized in the structural subnanovoid in the glass [21]. The pick-off annihilation rate of the o-Ps is related to the average size of the subnanovoids in fused silica [22,23]. In recent years, many significant results have been achieved by applying positron annihilation techniques into fused silica defect studies [24–26]. In this work, we attempt to characterize the microstructure defects variation in fused silica under different atmospheres annealing processes. For this purposes, we employed two different PAS techniques: Doppler broadening annihilation spectroscopy (DBS) coupled to a slow positron beam and Positron annihilation lifetime spectroscopy (PALS). The investigation of DBS coupled to a variable-energy slow positron beam is possible to provide a defect distribution from a few nanometers to several microns of the samples by tuning positron implantation energy from few eV to about 20 keV. The PALS is possible to detect defect information about one hundred microns in solid materials. In addition, we present the results of systematically studies on characteristics of microstructure defects. The obtained results can provide important information for understanding the laser damage mechanism of fused silica.

## 2. Experimental materials and methods

### 2.1. Sample preparation

In this section, the samples preparation is firstly presented and then, the details of PAS experiments are given. Fused silica samples (JGS1) with a dimension of 15 mm × 15 mm × 1 mm and a surface roughness of less than 1 nm RMS (root mean square) were used as substrates.

Samples of C1 were untreated fused silica samples. The other samples were isothermally annealed at 1000 K for 3 h in a furnace under an air atmosphere (C2), a vacuum atmosphere (C3) and a hydrogen atmosphere (C4), respectively. 5 K/min heating rate was used to the heating process. 5 K/min cooling rate with a temperature range from 1000 K to 500 K and natural cooling below 500 K

were applied. The details on the sample preparation are presented in Table 1.

### 2.2. Positron annihilation spectroscopy (PAS)

PAS experiments were done at room temperature. Two PAS techniques were employed to research defects in fused silica, using radioactive <sup>22</sup>Na isotopes as a positron source. The positron–electron annihilation in matter is completely dominated by the emission of two 511 keV photons in the opposite direction in the center-of-mass system. Since the momentum of the positron in the delocalized state is much lower than the electron moment in the solid material, the annihilation parameters such as Doppler-shift provide information on the electronic structure. Firstly, we discuss briefly the Doppler broadening positron annihilation spectra by measuring the 511 keV positron–electron pair annihilation line at room temperature coupled to a slow variable mono-energetic positron beam. The doppler broadening of the line positron annihilation is characterized by so called *S* and *W* parameters, which are defined as the ratio of the central region (511 ± 0.8 keV) and wing region ((511 ± 1.7 to 511 ± 3.1 keV) to the total area of the 511 keV annihilation peak, respectively. The *S*-parameter describes mainly annihilation with low momentum valence electrons. Correspondingly, *W*-parameter describes mainly annihilation with high momentum core electrons. Consequently, an increase (decrease) in *S* (*W*) parameter indicates the presence of vacancy type defects. The *S* and *W* values were recorded as a function of the positron implantation energy *E<sub>p</sub>* between 0.25 and 20.0 keV using a slow positron beam. For the keV energy of positron, the probability of its implantation depth is given by Refs. [27,28]:

$$P(z, E) = \frac{m[\rho I(1 + \frac{1}{m})]^m z^{m-1}}{(AE^n)^m} \exp\left\{-\frac{[\rho I(1 + \frac{1}{m})]^m z^m}{(AE^n)^m}\right\} \quad (1)$$

where *P* is the probability of positron implantation depth, *A* is the empirical parameters, *m* is the shape parameter, *z* is the depth from the surface in nm, *E* is the positron beam energy in keV and  $\rho$  is the material density in g/cm<sup>3</sup>. In addition, the empirical parameters and the density of fused silica are equal as follows: *A* = 40, *m* = 2, *n* = 1.6 and  $\rho$  = 2.2 g/cm<sup>3</sup>. Therefore, the positron mean implantation depth in fused silica varied from 0 to 2.2 μm by tuning positron implantation energy from few eV to 20 keV. The positron implantation depth profiles are represented in Fig. 1 for several positron incident energies in the range 1.5–20 keV. Therefore, Doppler broadening annihilation coupled to a slow positron beam is used to detect the surface state of the sample and the surface defect information of the polishing redeposition layer of fused silica.

As a second technique, we carried out the Positron annihilation lifetime experiments. The positron lifetime is measured as the time-interval between the detection of a 1.27 MeV γ-ray, which is emitted almost simultaneously with a positron in the decay of <sup>22</sup>Na, and the 511 keV γ-ray emitted as a by-product of the positron annihilation. The positron annihilation rate is proportional to the local electron density. Therefore, the measurement of the positron lifetime allows the distinction between annihilation of “free” positrons and positrons trapped in lattice defects such as vacancies. After subtracting the source and background components, the lifetime spectra were fitted to the following expression:

$$L(t) = \text{Re} \otimes \sum_i \frac{I_i}{\tau_i} \exp(-t/\tau_i) \quad (2)$$

where  $\tau_i$  is one of the lifetime components of the spectra, and *I<sub>i</sub>* is

**Table 1**  
Preparation conditions of fused silica samples.

Sample	Annealing atmosphere	Experiment parameter
C1	Untreated fused silica	/
C2	Air	/
C3	Vacuum	Vacuum pressure $P < 5 \times 10^{-4}$ pa
C4	Hydrogen	Closing the vacuum valve when the temperature rises to 1000 K, and then pass over the hydrogen with the pressure about 0.2 Mpa

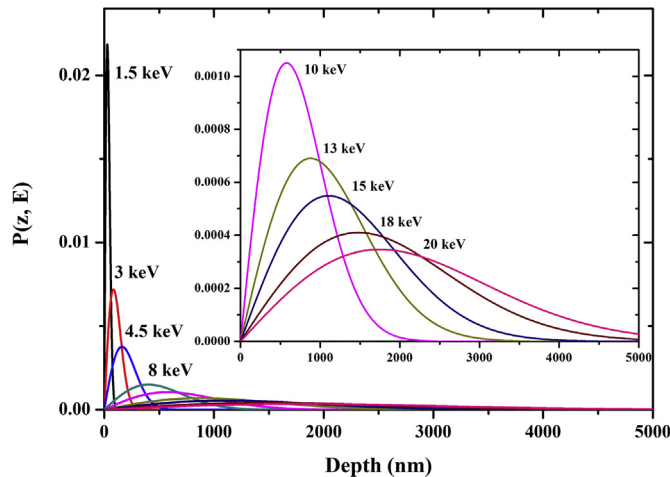


**Fig. 1.** Positron depth profile in fused silica calculated for indicated positron incident energies according to Ref. [27] and Ref. [28] with the parameters  $\rho = 2.2 \text{ g/cm}^3$ ,  $m = 2$ ,  $n = 1.6$ , and  $A = 40$ . The inset shows a zoom of the data in the main panel, for positron incident energies between 10 and 20 keV.

the corresponding intensity. Taking into account the convolution with the instrumental resolution  $Re$ , the experimental data can be fitted with several positron lifetime components by the software LIFETIME9 [29]. The lifetime of the positron is related to the defects, and it increases when the size or/and the concentration of defects increases. For three-component decomposition, we use:

$$L(t) = \text{Re} \otimes \left[ \frac{I_1}{\tau_1} \exp(-t/\tau_1) + \frac{I_2}{\tau_2} \exp(-t/\tau_2) + \frac{I_3}{\tau_3} \exp(-t/\tau_3) \right] \quad (3)$$

The maximum energy of positron obtained from  $^{22}\text{Na}$  radioactive source decay is 545 keV and the mean positron implantation depth in fused silica is about 110  $\mu\text{m}$ . This depth is approximatively consistent with the defect layer zone of fused silica [4]. Therefore, Positron annihilation lifetime spectroscopy is used to detect the defect information of the defect layer in fused silica.

### 3. Results and discussion

Fig. 2 shows the variation of the positron annihilation doppler broadening  $S$ -parameter as a function of incident positron beam energy  $E_p$  for the three samples. The variation of  $S$  at low energies ( $E < 1 \text{ keV}$ ) is due to the positron trapping at the surface. The starting value of the  $S$ -parameter corresponding to  $E_p = 0.25 \text{ keV}$ , is characteristic of the surface and this value is initially higher for C2 and C4 as compared with C1 and C3. With the increasing positron beam energy, positrons probe the polishing redeposition layer. For C1, the  $S$ -parameter initially increases steeply and it gradually keeps steady with the  $E_p > 6 \text{ keV}$ . In the case of C2, an initial

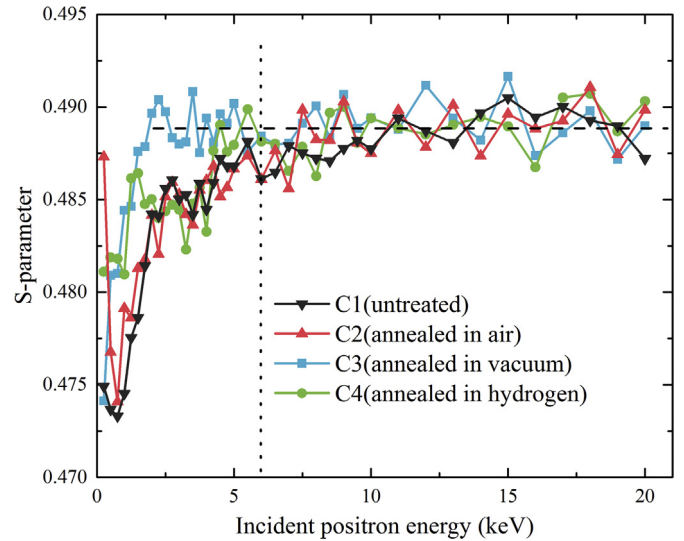


**Fig. 2.** The results of the variable mono-energy positron annihilation Doppler broadening spectroscopy experiments: Low momentum annihilation fraction  $S$ -parameter versus incident positron energy  $E_p$  for a series of fused silica samples (C1, C2, C3, and C4).

reduction sharply in  $S$ -parameter is observed and further, it holds a steeply increase between 1 and 6 keV, and gradually attains steady value beyond 6 keV. C3 show a similar behavior with C1 and the observed  $S$ -parameter value is higher than that of C1. For C4, the  $S$ -parameter initially increases steeply and it exhibits a broad minimum between 1 and 4 keV, beyond which it starts to increase and then gradually attains steady value beyond 5 keV.

The higher  $S$ -parameter with  $E_p < 1 \text{ keV}$  observed for annealed in air atmosphere samples (C2) as compared to untreated samples (C1) indicates that the surface state of the sample was changed after annealing in air atmosphere. The change is considered to be caused by contamination of the sample surface during the air atmospheric annealing process, and the surface chemical state affects the  $S$ -parameter [30,31]. In the oxygenated environment, high temperature annealing can reduce oxygen defects. However, positrons are not sensitive to positively charged oxygen defects as compared to neutral or negatively charged defects. There are no significant changes with the  $E_p > 1 \text{ keV}$  between C1 and C2, suggesting that annealing in air atmosphere has no significant effect on the defects (except positively oxygen defect) of the polishing redeposition layer in the sample.

$S$ -parameter of C3 is higher than that of C1. That is because some of the Si–O bonds on the surface of the C3 are broken in the vacuum atmosphere at 1000 K, and the NBOHC and oxygen-deficiency defects are generated [19,25,32]. Positrons are easily trapped by NBOHC and are more likely to annihilate with electrons at low valence that makes  $S$ -parameter increasing. Besides, the similar  $S$ -parameter with  $E_p < 1 \text{ keV}$  observed for C3 as compared to C1 indicates that there is no obvious pollution of the surface chemical state in the annealing process. That is because vacuum environment is cleaner than the atmospheric environment. There are no significant changes when positron energies exceed 6 keV, suggesting that the depth of influence under vacuum annealing parameters is about 300 nm (corresponding to positron energy below 6 keV).

C4 was annealed in hydrogen atmosphere without oxygen. Similar to C3, some of the Si–O bonds on the surface of the C4 are broken in the hypoxic environment at 1000 K, and the NBOHC and oxygen defects are generated. However, hydrogen atoms can fill

**Table 2**  
Positron lifetime results for fused silica with different annealing atmospheres.

Sample	$\tau_1$ (ps)	$I_1$ (%)	$\tau_2$ (ps)	$I_2$ (%)	$\tau_3$ (ps)	$I_3$ (%)	$R$ (nm)
C1	165.4	31.0	983.0	24.9	1633	44.1	0.2486
C2	160.6	30.7	789.0	16.89	1567	52.4	0.2413
C3	157.6	29.1	759.0	16.7	1560	52.6	0.2406
C4	154.4	30.7	713.0	15.0	1562	55.9	0.2408

monovacancies or other defects in the sample surface, and form new hydrogen interstitial defects [33]. This effect will reduce the positron capture efficiency and reduce the  $S$  parameter. Compared to C1, the  $S$  parameter of sample C4 is slightly higher in the surface and similar above 100 nm (Corresponding to positron energy about 2 keV). What's more, the higher  $S$ -parameter with  $E_p < 1$  keV observed for C4 as compared to C1 indicates that the surface chemical state of the samples was changed because the hydrogen is a reducing gas.

PAL experiments were performed at room temperature. Each spectrum was fitted by the LIFETIME 9 program with a three-component fitting procedure. The results of positron lifetime are presented in Table 2. The lifetime of the shortest component,  $\tau_1 \sim 160$  ps, is attributed to the lifetime component of the host which mainly reflects the normal Si–O–Si network structure and some short lifetime mono-vacancy defects. The second shorter component  $\tau_2$  can be ascribed to the annihilation of positrons trapped at defects. The long-lived lifetime component  $\tau_3$  is usually correlated to the pick-off annihilation of  $o$ -ps that is trapped in a void. Therefore,  $\tau_3$  can be related to the void radius. The void is assumed to be a spherical potential well surrounded by an electron layer of thickness  $\Delta R$ . Then  $\tau_3$  (ns) as a function of the void radius  $R$  (nm) is given by Refs. [21–23]:

$$\frac{1}{\tau_3} = 2 \times \left[ 1 - \frac{R}{R + \Delta R} + \frac{1}{2\pi} \sin\left(\frac{2\pi R}{R + \Delta R}\right) \right] \quad [4]$$

where  $\Delta R = 0.1656$  nm has been determined by fitting experimental  $\tau_3$  values to known void radii.

The changes of the lifetime component  $\tau_1$ ,  $\tau_2$  and corresponding intensity  $I_1$ ,  $I_2$  in different samples are shown in Fig. 3. The solid line is drawn in Fig. 3 for visual clarification only. After annealing, the  $\tau_1$  and  $I_1$  decrease lightly. It is because high temperature increases the energy of atomic motion. That makes the Si–O bond re-bonding and reduces NBOHCs [26,34,35]. Besides, due to the small volume and high diffusion coefficient of the hydrogen atom, the hydrogen

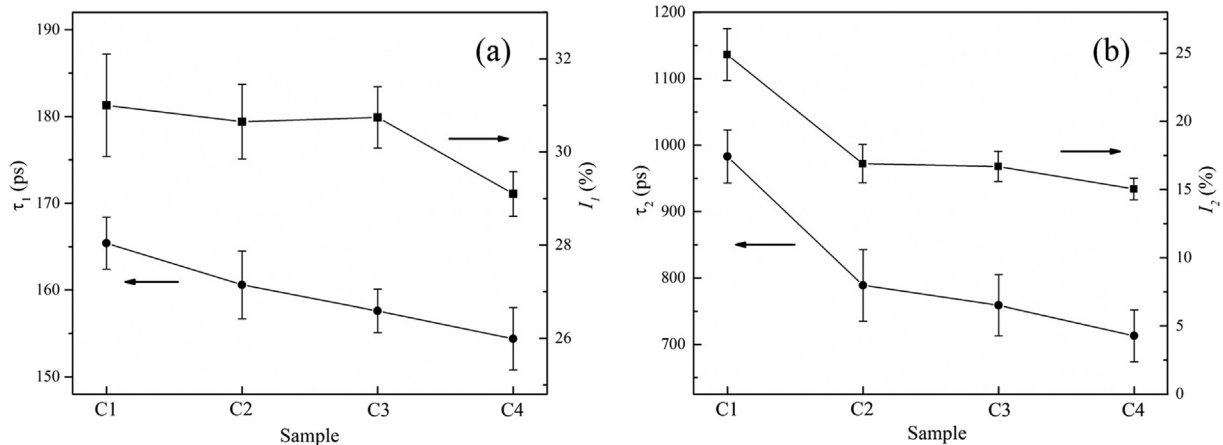


**Fig. 3.** Comparison of positron lifetime parameters (a)  $\tau_1$ ,  $I_1$  and (b)  $\tau_2$ ,  $I_2$  for a series of fused silica samples (C1, C2, C3, and C4).

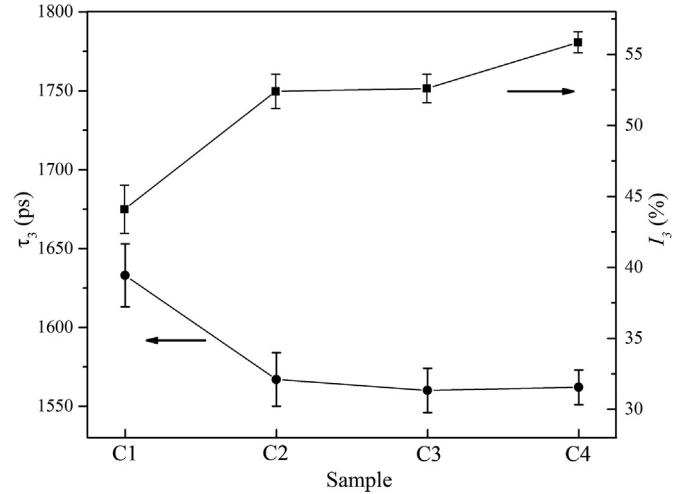


**Fig. 4.** Positron annihilation parameters  $\tau_3$  and  $I_3$  as a function of the fused silica samples (C1, C2, C3, and C4).

can diffuse into the defect layer and fill the vacancy defects in C4 (annealing in a hydrogen atmosphere). This decreases the positron trapping rate of the monovacancy defects, thus leading to a further reduction of the first positron lifetime and intensity. The  $\tau_2$  and  $I_2$  decrease obviously after annealing suggesting that the annealing treatment can significantly reduce the size and concentration of vacancy clusters. Due to the energy of atomic motion increased in high temperature, Si–O bond re-bonding makes some vacancy clusters decompose into small vacancy clusters and vacancy size defects [19,36]. In addition, an annealing process is considered to anneal out isolated point defects. This phenomenon leads to the reduction of the positron trapping concentration. The cluster defect is bound to some of the hydrogen atoms, which results in a slight decrease in the  $\tau_2$  and  $I_2$  of the C4 (annealing in a hydrogen atmosphere).

Fig. 4 shows the results of the third-lifetime component  $\tau_3$  and relative intensity  $I_3$  for fused silica samples annealing under different atmosphere. The  $\tau_3$  decreases after annealing suggesting that the void size becomes smaller [25]. The results show that the high temperature annealing makes some non-bridging oxygen bonds combine with oxygen. Therefore, 3- or 4-membered rings rearrange into larger rings, such as 6-membered ones, which leads to the compression of the void size [25,37]. There is no obvious

difference between the samples annealed in a hydrogen atmosphere and the samples annealed in other atmospheres for  $\tau_3$ , which indicates that the hydrogen atoms have no effect on the large voids. The  $I_3$  increases after annealing suggesting that the relative concentration of structure voids is significantly increased.  $I_3$  of C4 increased significantly higher than that of C2 and C3, this is because the hydrogen can penetrate into the single vacancy defects that leads to a significant decrease of the  $I_1$ . The intensity of the positron lifetime is a relative concept, even if there is no significant change in the void concentration in the sample, the significant decline in the  $I_1$  makes  $I_3$  increase significantly [30].

#### 4. Conclusions

Two PAS techniques were employed to research the microstructure variation of the vacancy clusters and the structure voids in the polishing redeposition layer and the defect layer of fused silica under different annealing atmospheres. The microstructure of fused silica shows different changes after annealing. The lifetimes and their relative intensities of the samples C2 and C3 that annealed in the air and the vacuum are approximately equal. These experimental results indicate that the ambient oxygen atmosphere does not affect the defect layer. In other words, due to the large volume and low diffusion coefficient of the oxygen atom, the ambient oxygen atmosphere only affects the surface of the sample (about 300 nm depth). In the case of the sample C4 that annealed in the hydrogen atmosphere, the  $\tau_1$  and  $I_1$  change significantly compared to the sample C2 and C3, which indicates that the hydrogen atoms can penetrate into the defect layer inside the sample and then affect the defect layer. Besides, the hydrogen atoms that penetrate into the defect layer have an influence on vacancy defects and vacancy clusters, while having no effect on the large voids. The DBS results show that the NBOHC and oxygen-deficiency defects are generated in the surface (about 300 nm depth) of fused silica after annealing in a vacuum atmosphere and a hydrogen atmosphere. The PALS results suggest that the NBOHC and the vacancy clusters in the defect layer of fused silica are significantly reduced by annealing treatment. The compression of the void size in the defect layer by annealing process are also observed by the PALS. These experimental results can provide important information for understanding the laser damage mechanism and improving laser damage resistance properties of the fused silica optics.

#### Acknowledgements

This work was supported by the Young Scientists Fund of the National Natural Science Foundation of China [grant numbers 11404301, 61505185].

#### References

- [1] J. Neauport, L. Lamaignere, H. Bercegol, *Opt. Express* 13 (2005) 0163–10171.
- [2] F. Génin, K. Michlitsch, J. Furr, *Proc. SPIE* 2996 (1997) 126–138.
- [3] Q. Zhu, W. Zheng, X. Wei, F. Jing, D. Hu, W. Zhou, B. Feng, J. Wang, Z. Peng, L. Liu, Y. Chen, L. Ding, D. Lin, L. Guo, Z. Dang, W. Deng, *Proc. SPIE* 8786 (2013) 87861G.
- [4] D.W. Camp, M.R. Kozłowski, L.M. Sheehan, M. Nichols, M. Dovik, R. Raether, I. Thomas, *Proc. SPIE* 3244 (1998) 356–364.
- [5] N. Shen, M.J. Matthews, S. Elhadj, P.E. Miller, A.J. Nelson, J. Hamilton, *J. Phys. D: Appl. Phys.* 46 (2013) 165305.
- [6] M.J. Matthews, C.W. Carr, H.A. Bechtel, R.N. Raman, *Appl. Phys. Lett.* 99 (2011) 151109.
- [7] R.N. Raman, M.J. Matthews, J.J. Adams, S.G. Demos, *Opt. Express* 18 (2010) 15207.
- [8] J. Wong, J.L. Ferriera, E.F. Lindsey, D.L. Haupt, I.D. Hutcheon, J.H. Kinney, *J. Non Cryst. Solids* 352 (2006) 255–272.
- [9] S.O. Kucheyev, S.G. Demos, *Appl. Phys. Lett.* 82 (2003) 3230–3232.
- [10] S.Z. Xu, X.D. Yuan, X.T. Zu, H.B. Lv, X.D. Jiang, L. Zhang, W.G. Zheng, *J. Non Cryst. Solids* 353 (2007) 4212–4217.
- [11] N. Shen, P.E. Miller, J.D. Bude, T.A. Laurence, T.I. Suratwala, W.A. Steele, M.D. Feit, L.L. Wong, *Opt. Eng.* 51 (2012) 121817.
- [12] W. Deng, J.T. Guo, R.S. Brusa, G.P. Karwasz, A. Zecca, *Mater. Lett.* 59 (2005) 3389–3392.
- [13] M.J. Puska, R.M. Nieminen, *Rev. Mod. Phys.* 66 (1994) 841.
- [14] D. Chaudhary, M.R. Went, K. Nakagawa, S.J. Buckman, J.P. Sullivan, *Mater. Lett.* 64 (2010) 2635–2637.
- [15] L.J. Zhang, T. Wang, L.H. Wang, J.D. Liu, M.L. Zhao, B.J. Ye, *Scr. Mater.* 67 (2012) 61–64.
- [16] K. Ito, H. Nakanishi, Y. Ujihira, *J. Phys. Chem. B* 103 (1999) 4555–4558.
- [17] D.W. Gidley, W.E. Frieze, T.L. Dull, A.F. Yee, E.T. Ryan, H.M. Ho, *Phys. Rev. B* 60 (1999) 5157–5160.
- [18] K. Ciesielski, A.L. Dawidowicz, T. Goworek, B. Jasinska, J. Wawryszczuk, *Chem. Phys. Lett.* 289 (1998) 41–45.
- [19] S. Dannefaer, T. Bretagnon, D. Kerr, *J. Appl. Phys.* 74 (1993) 884–890.
- [20] H. Saito, T. Hyodo, *Phys. Rev. Lett.* 90 (2003) 193401(4).
- [21] Y. Sasaki, Y. Nagai, H. Ohkuboa, K. Inoue, Z. Tangb, M. Hasegawa, *Radiat. Phys. Chem.* 68 (2003) 569–572.
- [22] S.J. Tao, *J. Chem. Phys.* 56 (1972) 5499–5510.
- [23] M. Eldrup, *Chem. Phys.* 63 (1981) 51–58.
- [24] K. Ito, T. Oka, Y. Kobayashi, Y. Shirai, K. Wada, M. Matsumoto, M. Fujinami, T. Hirade, Y. Honda, H. Hosomi, Y. Nagai, K. Inoue, H. Saito, K. Sakaki, K. Sato, A. Shimazu, A. Uedono, *J. Appl. Phys.* 104 (2008) 026102.
- [25] M. Ono, K. Hara, M. Fujinami, S. Ito, *Appl. Phys. Lett.* 101 (2012) 164103.
- [26] C. Li, W. Zheng, Q. Zhu, J. Chen, B.Y. Wang, X. Ju, *Nucl. Instr. Meth. Phys. Res. B* 384 (2016) 23.
- [27] S. Valkealahti, R.M. Nieminen, *Appl. Phys. A* 32 (1983) 95–106.
- [28] S. Valkealahti, R.M. Nieminen, *Appl. Phys. A* 35 (1984) 51–59.
- [29] J. Kansy, *Nucl. Instr. Meth. Phys. Res. A* 374 (1996) 235.
- [30] R.K. Rehberg, H.S. Leipner, *Positron Annihilation in Semiconductors*, Springer Verlag, Berlin, 1998.
- [31] P.G. Coleman, *Positron Beams and Their Applications*, World Scientific, Singapore, 2000.
- [32] M. Sometani, R. Hasunuma, M. Ogino, H. Kuribayashi, Y. Sugahara, A. Uedono, K. Yamabe, *Jpn. J. Appl. Phys.* 51 (2012) 021101.
- [33] P.H. Leo, K.D. Moore, P.L. Jones, F.H. Cocks, *Phys. Status Solidi B* 108 (1981) K145–K149.
- [34] M. Hasegawa, M. Saneyasu, M. Tabata, Z. Tang, Y. Nagai, T. Chiba, Y. Ito, *Nucl. Instrum. Methods Phys. Res. B* 166–167 (2000) 431–439.
- [35] R.S. Brusa, S. Mariuzzi, L. Ravelli, P. Mazzoldi, G. Mattei, W. Egger, C. Hugenschmidt, B. Löwe, P. Pikart, C. Macchi, A. Somoza, *Nucl. Instrum. Methods Phys. Res. B* 268 (2010) 3186–3190.
- [36] M.A. Stevens-Kalceff, *Phys. Rev. Lett.* 84 (2000) 3137.
- [37] A.E. Geissberger, F.L. Galeener, *Phys. Rev. B* 28 (1983) 3266.